Multi-Sensor Investigation of Large Ice Particles Using GPM and NASA GV Data

Randy J. Chase[1], Stephen W. Nesbitt[1], Paloma Borque[1], Joe Finlon[1] and Greg M. McFarquhar[2]

[1]Department of Atmospheric Sciences, University of Illinois at Urbana-Champaign, Urbana, IL, USA

[2]CIMMS/School of Meteorology, University of Oklahoma, Norman, OK, USA

1. Motivation

Globally, where are large ice particles found?

For what meteorological conditions are large ice particles found?

What types of ice hydrometeors are found?

Since a wide variety of ice particle shapes and sizes exist in the atmosphere, understanding the global distribution of precipitating ice characteristics will help constrain *a priori* assumptions about particle terminal fall speed and effective density in global retrievals of snowfall rate (S) and ice water content (IWC).

2. flagHeavyIcePrecip

Iguchi et al. (2018) introduced a flag retrieved from GPM-DPR data that identifies profiles where GPM-DPR is most likely sampling large or intensely precipitating ice particles. The following criteria has to be met anywhere in the column:

$$Z_{Ku} \geq 27\ dBZ$$

$$DFR_{Ku-Ka} \geq 7\ dB$$

$$T \leq -10\ ^{\circ}\mathrm{C}$$

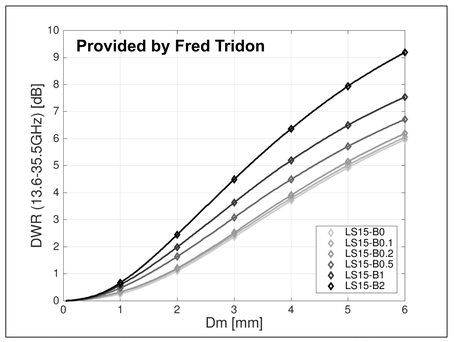

Fig 1. Forward modeled dual-wavelength ratios (same as DFR) as a function of mass weighted mean diameter using the DDA calculations from Leinonen and Szyrmer (2015).

Basic Principal:
Larger DFR's are a result of larger particles (ignoring attenuation due to liquid water and non-uniform beam filling)

What is meant by 'Large'?
In Iguchi et al. (2018) no formal size of particles are associated with the conditions above, but considering DDA scattering results from Leinonen and Szyrmer (2015) mass weighted diameter (Dm, Fig 1) values are ≥ 4 mm.

2a. Caveat: GPM-DPR Ku Sidelobes

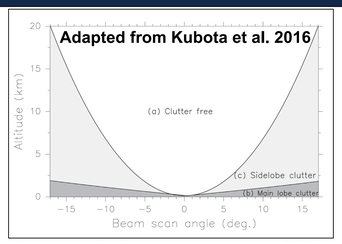

Fig 2. Ku-Clutter diagram from Kubota et al. (2016)

- Use of the measured reflectivity is required in order isolate the particle size effect on DFR without any assumptions of attenuation correction (attenuation should be low in ice for Ku and Ka), unfortunately that means clutter is possible in the Ku-band data
- Kubota et al. (2016) showed this clutter and provided a solution to correcting the clutter (Fig 2)
- However, Fig 3a provides an example of clutter in DPR V05A that has not been mitigated in the GPM-DPR algorithms (~ 1 km)
- This example is from near Antarctica in SH winter, where the temperature profile allows the low level clutter to be found with $T \leq -10\ ^{\circ}\mathrm{C}$
- It is hypothesized the edge high frequencies of occurrence in Fig 4 (e.g. $-65\ ^{\circ}\mathrm{S}, 120^{\circ}\mathrm{E}$ to $180\ ^{\circ}\mathrm{E}$) are a result of classification of Ku-band clutter as large ice particles.

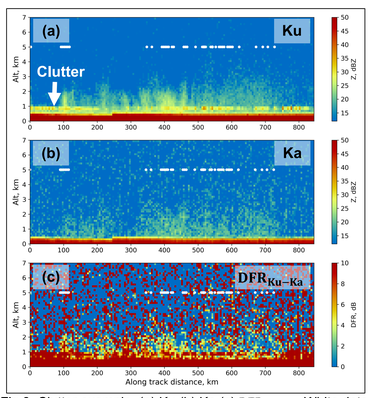

Fig 3. Clutter example. (a) Ku (b) Ka (c) DFR_{Ku-Ka}. White dots at 5 km are where flagHeavyIcePrecip is set. Ku-Crossray 29

3. Global Occurrence of Large Ice

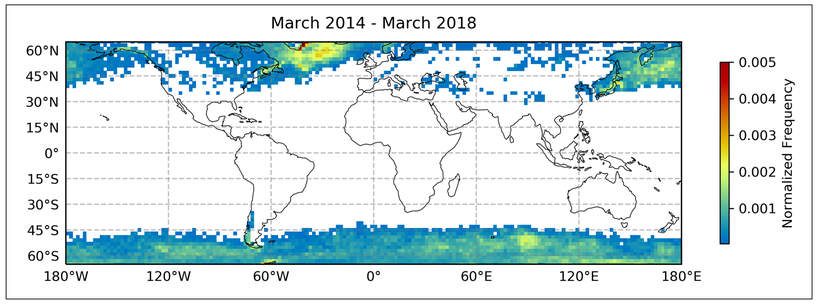

Fig 4. 1x1 degree of flagHeavyIcePrecip frequency of occurrence for surface $T \leq 1\ ^{\circ}\mathrm{C}$, normalized by total number of samples in each bin. Gates with less than 30 occurrences are masked. Total number of flagHeavyIcePrecip occurrence is 1,060,758

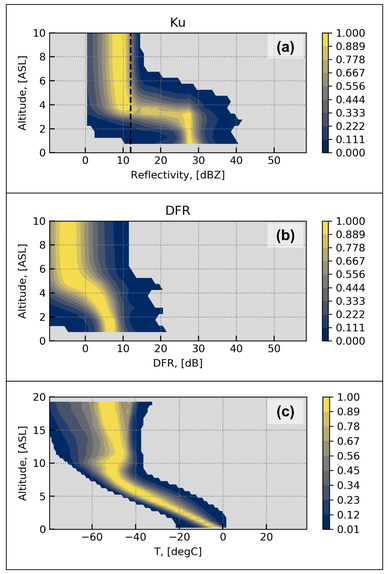

Fig 5. Contoured Frequency by Altitude Diagrams for the entire domain found in Fig 4. (a) Ku-band reflectivity, (b) DFR_{Ku-Ka} (c) MERRA-2 Temperature.

- 4 Years of GPM-DPR data show flagHeavyIcePrecip occurrence peaks mainly over high latitude oceanic regions (Fig 4), *although see section 2a*
- CFAD of Ku-band reflectivity show potential structure of reflectivity within flagHeavyIcePrecip profiles, with echo-tops near 4 km. Note: 12 dBZ minimum sensitivity for GPM-DPR (Fig 5a)
- CFAD of DFR_{Ku-Ka} indicates monotonically increasing values towards lower altitudes suggesting increasing particle size towards the surface (Fig 5b)
- CFAD of MERRA-2 matched temperature profiles show a profile with an average lapse rate of $8\ ^{\circ}\mathrm{C\ km^{-1}}$, suggesting frequent conditional instability (Fig 5c)

4. GPM/CloudSat Case: 30 Jan 2016

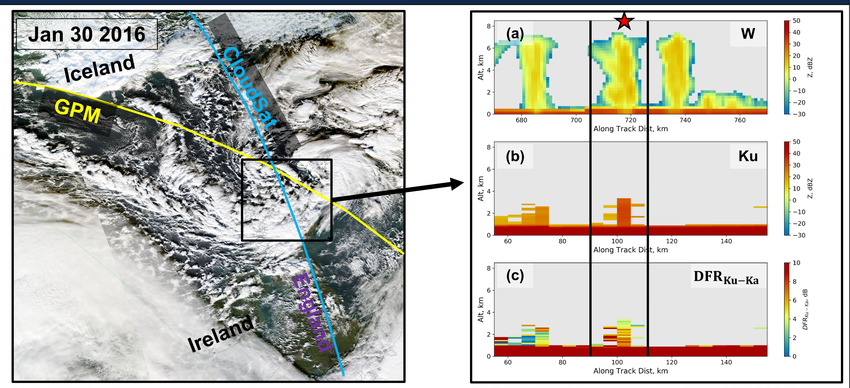

Fig 6. MODIS visible imagery courtesy of worldview.earthdata.nasa.gov. Blue line is CloudSat nadir beam. Yellow Line is GPM nadir beam.

Fig 7. (a) CloudSat W-band reflectivity (b) GPM-DPR Ku-band reflectivity (c) GPM-DPR DFR_{Ku-Ka}. Red star indicates the profile where the flagHeavyIcePrecip is set.

- An example of flagHeavyIcePrecip from the North Atlantic shows oceanic convection with overshooting tops (Fig 6)
- Profiles of CloudSat W-band reflectivity show the spatial structure of the deep cloud, extending up to the tropopause (Fig 7a)
- GPM-DPR conveys a much different scene with echo tops ≤ 4 km because of limited sensitivity and along track resolution, but flagHeavyIcePrecip is satisfied (Fig 7bc)
- MERRA-2 sounding exhibits moist-adiabatic lapse rates from LCL to tropopause (not shown)

5. OLYMPEX Case: 04 Dec 2015

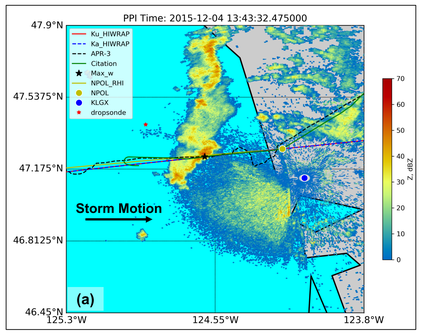

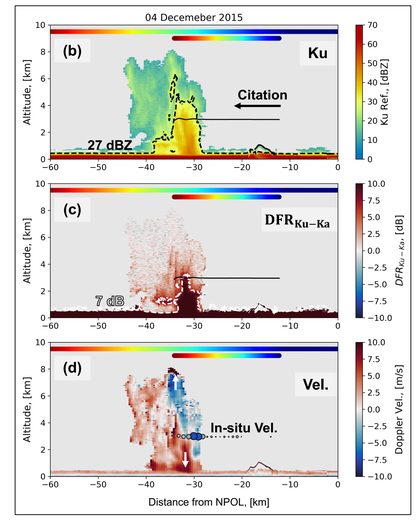

Fig 8. (a) 0.5 deg PPI Scan from KLGX at 13:43 with overlayed flight tracks from NASA DC-8 (Dashed Black), NASA ER-2 (Red/Blue), UND Citation (Green). (b) Cross sections of reflectivity, (c) DFR_{Ku-Ka}, (d) Vel. measured by the APR-3. Rainbow lines at 9.5 and 9 km indicate the APR-3 and UND Citation times respectively. (e) HVPS3 images from 13:43:44 UTC located spatially near -30 km

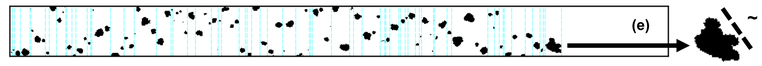

- An analogous example of flagHeavyIcePrecip was collected during OLYMPEX on 04 Dec 2015. Post-frontal convection was sampled off the coast of Washington State (Fig 8)
- PPI S-band radar scans show a quasi-linear rain band approaching the coast (Fig 8a)
- APR-3 Ku-, Ka- band radar shows the vertical structure of the storm with a convective and stratiform region (Melting Level ~1 km, Fig 8b)
- The UND Citation in-situ plane flying at $-12\ ^{\circ}\mathrm{C}$ recorded $10\ \mathrm{m\ s^{-1}}$ updrafts, LWC $> 1\ \mathrm{g\ m^{-3}}$ and copious graupel (Fig 8de)
- The flagHeavyIcePrecip conditions are set and are associated with large rimed particles producing the large DFR (Fig 8e)

6. Conclusions

1) 4-years of GPM-DPR flagHeavyIcePrecip are frequently found over high latitude oceans (Fig 4); although clutter needs to be better considered

2) Considering CFADs of T, profiles seem to be conditionally unstable suggesting the large ice particles are potentially being produced by upright convection (Fig 5c)

3) A case study using GPM-DPR, CloudSat and MODIS, show full tropospheric convection producing large ice with an MERRA-2 profile that is mostly moist adiabatic (Fig 6,Fig 7)

4) A case study from OLYMPEX provides insight of particle types in cold season oceanic convection (potentially analogous to storms producing flagHeavyIcePrecip), which are rimed, graupel-like particles. (Fig 8)

References

Iguchi, T., Kawamoto, N. and Oki, R., 2018: Detection of Intense Ice Precipitation with GPM/DPR. *J. Atmo. Ocean. Tech.;* Kubota, T., Iguchi, T., Kojima, M., Liao, L., Masaki, T., Hanado, H., Meneghini, R. and Oki, R., 2016: A Statistical Method for Reducing Sidelobe Clutter for the Ku-band Precipitation Radar on board the GPM *Core Observatory*. *J. Atmo. Ocean. Tech.*; Leinonen, L. and Szyrmer, W., 2015: Radar Signatures of Snowflake Riming: A Modeling Study. *Earth and Space Science*.

Acknowledgments

Funding from National Aeronautics and Space Administration, Precipitation Measurement Missions and NESSF (grants: NNX16AB70G and NNX16AD80G)